Quantum theory of luminescence in multiple-quantum-well Bragg structures

M. Schäfer,* M. Werchner, W. Hoyer, M. Kira, and S. W. Koch
Department of Physics and Material Sciences Center, Philipps-University, Renthof 5, D-35032 Marburg, Germany
(Received 12 June 2005; published 19 October 2006)

The quantum emission in radiatively coupled semiconductor multiple-quantum-well structures is investigated theoretically. It is shown that coupling effects can lead to a subradiant suppression of the emission compared to the emission of a single quantum well (QW). The suppression strength depends on the number and spacing of the QWs as well as on the homogeneous broadening and leads to an enhancement of the radiative lifetime of excitons in the structure. The strongest lifetime enhancement is found for Bragg-arranged QWs with small homogeneous broadening. Additionally, the radiative coupling between the QWs provides an exciton pumping mechanism such that excitons can directly be created into the state that has vanishing center-of-mass momentum.

DOI: 10.1103/PhysRevB.74.155315 PACS number(s): 78.67.De, 78.20.Bh, 78.55.Cr, 71.35.−y

I. INTRODUCTION/MOTIVATION

In the past decades, direct band-gap semiconductor quantum-wells (QWs) have been objects of great interest in solid state physics due to their reduced dimensionality and the relatively easy fabrication. In comparison to bulk semiconductors, the QW optical properties are often different as the carriers are confined in the direction perpendicular to the QW plane.[1,2] For example, QWs show the decay of electronic excitations while in bulk semiconductors polaritons are formed.[3,4] This decay is caused by Coulomb-mediated radiative recombination of electrons and holes and leads to a strong emission below the fundamental band gap at excitonic resonances even when true exciton populations, i.e., Coulomb-bound electron-hole pairs, are not present.[5] However, it is possible to distinguish between the emission from excitons and other electronic excitations with the help of photoluminescence (PL) spectra.[6] If excitons are formed, the recombination of carriers leads to a rapid decay of low-momentum excitons on a 10-picosecond time scale in a single QW.[7–9] This property is clearly undesirable in many situations, e.g., when Bose-Einstein condensation is pursued. Therefore, it is interesting to search for situations where the lifetime of the low-momentum excitons is enhanced and their recombination is suppressed.

Compared to a single QW, a periodic and parallel alignment of two or more QWs can lead to new intriguing effects such as superradiance,[10–13] solitons,[14–16] the splitting of emission peaks,[17,18] and modified Rabi intersubband oscillations.[19,20] The origin of these effects is the optical coupling between the QWs which is caused by the virtual emission and reabsorption of photons within the multiple-quantum-well (MQW) system. The coupling strength is dependent on the spacing between the QWs and in general is strongest for Bragg structures, i.e., for QW spacings equaling one half of the wavelength of the 1*s*-exciton resonance.[21] In the present paper, we show that under appropriate conditions, i.e., at low carrier densities, the coupling between the QWs can lead to the overall suppression of emission in the MQW system, which then results in an enhancement of the lifetime of the electronic excitations.

In order to describe the radiative coupling in MQW systems, one has to distinguish between the driven excitonic polarization and incoherent excitons. Optical excitation induces an interband polarization which is coherent such that all microscopic transitions carry the same phase. Due to scattering processes, these quantities lose their phase information on a typical time scale of a few picoseconds. Once a purely incoherent situation is reached, it is characterized by a generally complicated many-body state of electrons, holes, excitons, and other quasiparticles. In this limit, the expectation value of the electric field vanishes, i.e., there is no classical light, and all radiation is incoherent PL. The light emission properties are then exclusively determined by the quantum fluctuations. Therefore, a quantum description of the light field is absolutely essential. A theory providing such a description has been derived in Ref. 22. In this paper, we extend this approach to describe both exciton populations and radiative coupling effects in MQW systems. We evaluate the MQW PL under several different experimentally relevant conditions and discuss how subradiant suppression of PL and exciton decay can be realized. We also show how coupled QWs can be used to pump excitons via their radiative coupling.

The paper is structured as follows. We introduce the underlying theory and present the equations of motion describing the system, in Sec. II. With the help of these equations, we investigate the suppression of PL in a system consisting of N QWs and explain its microscopic origin in Sec. III. In particular, we study the dependence of the emitted light intensity on the number of QWs and their spacing. Additionally, we explain how the emission strength is related to the radiative recombination of incoherent quasiparticles and, especially, to the radiative lifetime of excitons. In Sec. IV, we study the possibilities for directly tailoring the radiative exciton lifetime, and show in Sec. V that the radiative coupling provides a mechanism to directly excite true exciton populations.

II. MICROSCOPIC THEORY

Since we are interested in the quantum emission of a system of radiatively coupled QWs, we assume entirely incoherent conditions. In this limit, no optical polarization is present and the expectation value of the classical electric

field is zero. This describes an excited semiconductor after electrical pumping or after optical coherences have dephased on a picosecond-time scale. In order to systematically treat the MQW coupling effects, we start from the fully microscopic carrier-photon system including light-matter and Coulomb interaction as discussed, e.g., in Ref. 22.

This theory describes all carriers in the investigated system via fermionic electron annihilation and creation operators $a_{m,\lambda,\mathbf{k}}$ and $a^{\dagger}_{m,\lambda,\mathbf{k}}$, where the momentum of the Bloch electrons is given by $\hbar\mathbf{k}$ and the band index by λ. The additional index m denotes the label of the QW in which the electron is annihilated or created. For sufficiently narrow QWs, the carriers are strongly confined in the direction perpendicular to the QWs such that only the lowest confinement level has to be considered. Hence, we restrict the analysis to two-band situations with one valence and one conduction band. Additionally, we concentrate on pure radiative coupling effects and assume the QW spacing Δs to be large enough to prevent electronic coupling between the carriers in different QWs. This is justified for the QW spacings that are interesting for radiative coupling, i.e., Δs is of the order of the wavelength of light which is large compared to the de Broglie wavelength defining the typical electronic coupling distance.

The light field is quantized via bosonic annihilation and creation operators $B_{\mathbf{q},q_\perp}$ and $B^{\dagger}_{\mathbf{q},q_\perp}$ for each light mode $(\mathbf{q},q_\perp)$. Due to the symmetry of the setup, it is useful to divide the wave vector into an in-plane component $\mathbf{q}$ (momentum parallel to the QW plane) and a perpendicular component $q_\perp$ (momentum in the direction perpendicular to the QWs). Here the three-dimensional photon wave vector $(\mathbf{q},q_\perp)$ includes information about the angle of incidence as well as the frequency of the light ω_q with $q=|\sqrt{\mathbf{q}^2+q_\perp^2}|$.

As shown previously,[22] the Coulomb interaction as well as the light-matter interaction lead to an infinite hierarchy of coupled equations of motion which can be truncated systematically with the help of the cluster-expansion formalism.[23–25] Here, we truncate the hierarchy at the $\langle 6\rangle$-point level such that single-particle contributions and two-particle correlations are fully taken into account. This leads to the semiconductor luminescence equation (SLE) which describes carriers, excitons, and photon correlations at an equivalent level. Since the derivation of the SLE without excitonic correlations for a single QW was already performed in Refs. 22 and 26, we concentrate here on the elements critical for MQW PL.

The fundamental quantity for the computation of the PL is the rate of the emitted photons. The photon number is given by the diagonal part of the expectation value

$$\langle B^{\dagger}_{\mathbf{q},q_\perp} B_{\mathbf{q}',q'_\perp}\rangle = \Delta\langle B^{\dagger}_{\mathbf{q},q_\perp} B_{\mathbf{q}',q'_\perp}\rangle + \langle B^{\dagger}_{\mathbf{q},q_\perp}\rangle\langle B_{\mathbf{q}',q'_\perp}\rangle \tag{1}$$

which can be factorized into two parts. The second term on the right-hand side corresponds to the classical intensity $\langle|E|^2\rangle$ such that the "Δ" is related to the difference $\langle E^2\rangle - \langle E\rangle^2$ and thus labels pure quantum correlations. The equation of motion for this quantity yields

$$\begin{aligned} i\hbar\frac{\partial}{\partial t}\Delta\langle B^{\dagger}_{\mathbf{q},q_\perp} B_{\mathbf{q}',q'_\perp}\rangle &= (\hbar\omega_{q'} - \hbar\omega_q)\Delta\langle B^{\dagger}_{\mathbf{q},q_\perp} B_{\mathbf{q}',q'_\perp}\rangle \\ &+ i\sum_{m,\mathbf{k}} \mathcal{F}^{\star}_{m,\mathbf{q}',q'_\perp}\Pi^{\mathbf{k},m}_{\mathbf{q},q_\perp} \\ &+ i\sum_{m,\mathbf{k}} \mathcal{F}_{m,\mathbf{q},q_\perp}(\Pi^{\mathbf{k},m}_{\mathbf{q}',q'_\perp})^{\star}, \end{aligned} \tag{2}$$

where the photon energy is denoted by $\hbar\omega_q$. The quantized light field is coupled to photon-assisted polarizations

$$\Pi^{\mathbf{k},m}_{\mathbf{q},q_\perp} \equiv \Delta\langle B^{\dagger}_{\mathbf{q},q_\perp} a^{\dagger}_{m,v,\mathbf{k}} a_{m,c,\mathbf{k}+\mathbf{q}}\rangle, \tag{3}$$

which describe a transition amplitude of a correlated process where a photon is emitted while an electron-hole pair recombines. The strength of the light-matter coupling is defined by $\mathcal{F}_{m,\mathbf{q},q_\perp} \equiv d_{cv}\mathcal{E}_q U_{m,\mathbf{q},q_\perp}$ that contains the dipole matrix element d_{cv} between conduction and valence band, the vacuum field amplitude $\mathcal{E}_q = \sqrt{\frac{\hbar\omega_q}{2\varepsilon_0}}$ as well as the overlap integral $U_{m,\mathbf{q},q_\perp} = \int g_m(z) u_{\mathbf{q},q_\perp}(z) dz$ between the mode function $u_{\mathbf{q},q_\perp}(z)$ and the confinement function $g_m(z)$ of QW m. Since the confinement function is very narrow compared to the optical wavelength, we can assume that $g_m(z)$ is δ-function-like. Therefore, only the mode function at the QW position is relevant. The mode functions contain all information about the photonic environment. In realistic systems, this environment can be given by buffer layers separating the QWs and substrate or air surrounding the sample. Furthermore, the surfaces between air and substrate are often cladded by antireflection coating layers. In our model, we assume the QW environment to be optically inactive and we treat it as a frequency-independent background refractive index n which enters the mode functions via transmission and reflection coefficients.[22]

The dynamics of the photon-assisted polarization is given by the semiconductor luminescence equation (SLE)

$$\begin{aligned} i\hbar\frac{\partial}{\partial t}\Pi^{\mathbf{k},m}_{\mathbf{q},q_\perp} &= (\tilde{\epsilon}^{m}_{\mathbf{k},\mathbf{q}} - \hbar\omega_{\mathbf{q}})\Pi^{\mathbf{k},m}_{\mathbf{q},q_\perp} - (1 - f^{e,m}_{\mathbf{k}+\mathbf{q}} \\ &- f^{h,m}_{\mathbf{k}})\sum_{\mathbf{k}'} V_{\mathbf{k}-\mathbf{k}'}\Pi^{\mathbf{k},m}_{\mathbf{q},q_\perp} + i\mathcal{F}_{m,\mathbf{q},q_\perp}\Omega^{\mathrm{SE}}_{m}(\mathbf{k},\mathbf{q}) \\ &+ i\Omega^{\mathrm{RC}}_{m}(\mathbf{k},\mathbf{q},q_\perp) - (1 - f^{e,m}_{\mathbf{k}+\mathbf{q}} \\ &- f^{h,m}_{\mathbf{k}})\Delta\langle B^{\dagger}_{\mathbf{q},q_\perp} B_{\mathbf{q}\Sigma_m}\rangle + i\hbar\frac{\partial}{\partial t}\Pi^{\mathbf{k},m}_{\mathbf{q},q_\perp}|_{\mathrm{scatt}}, \end{aligned} \tag{4}$$

with the Coulomb-renormalized single-particle energies

$$\tilde{\epsilon}^{m}_{\mathbf{k},\mathbf{q}} = \epsilon^{c}_{m,\mathbf{k}+\mathbf{q}} - \epsilon^{v}_{m,\mathbf{k}} - \sum_{\mathbf{k}'} V_{\mathbf{k}-\mathbf{k}'}(f^{e,m}_{\mathbf{k}'+\mathbf{q}} + f^{h,m}_{\mathbf{k}'}), \tag{5}$$

where $V_{\mathbf{k}}$ denotes the Coulomb matrix element in momentum space. The electron and hole contributions enter via

$$f^{e,m}_{\mathbf{k}} = \langle a^{\dagger}_{m,c,\mathbf{k}} a_{m,c,\mathbf{k}}\rangle \tag{6}$$

$$f_{\mathbf{k}}^{h,m} = 1 - \langle a_{m,v,\mathbf{k}}^{\dagger} a_{m,v,\mathbf{k}} \rangle. \tag{7}$$

In Eq. (4), the Coulomb sum over Π provides excitonic resonances to the photon-assisted polarizations. The spontaneous recombination processes are driven via

$$\Omega_m^{\mathrm{SE}}(\mathbf{k},\mathbf{q}) = f_{\mathbf{k}+\mathbf{q}}^{e,m} f_{\mathbf{k}}^{h,m} + \sum_{\mathbf{l}} c_{Xm,m}^{\mathbf{q},\mathbf{k},\mathbf{l}}, \tag{8}$$

where $f^e f^h$ describes the uncorrelated electron-hole plasma contribution and the second term contains the two-particle correlations $c_{Xm',m}^{\mathbf{q},\mathbf{k}',\mathbf{k}} = \Delta\langle a_{m,c,\mathbf{k}}^{\dagger} a_{m',v,\mathbf{k}'}^{\dagger} a_{m',c,\mathbf{k}'+\mathbf{q}} a_{m,v,\mathbf{k}-\mathbf{q}} \rangle$. Equation (8) includes two-particle correlations with equal QW indices $m=m'$. They can describe correlated plasma as well as exciton populations in QW m. Due to the structure of the spontaneous emission, also an uncorrelated electron-hole plasma can fundamentally be the origin of excitonic luminescence[5,6,27,28] and therefore excitonic luminescence does not need to be a signature of excitons in the system. Two-particle correlations with different QW indices, $m \neq m'$, determine the correlations of electron-hole pairs in different QWs and enter via the recombination correlation

$$\Omega_m^{\mathrm{RC}}(\mathbf{k},\mathbf{q},q_\perp) = \sum_{m \neq m'} \mathcal{F}_{m,\mathbf{q},q_\perp} \sum_{\mathbf{l}} c_{Xm',m}^{\mathbf{q},\mathbf{k},\mathbf{l}}, \tag{9}$$

which clearly couples different QWs. The MQW coupling is further modified by a stimulated contribution term $\Delta\langle B_{\mathbf{q},q_\perp}^{\dagger} B_{\mathbf{q}\Sigma_m} \rangle$, where the collective photon operator $B_{\mathbf{q},\Sigma_m} = \Sigma_{q_\perp'} i\mathcal{F}_{m,\mathbf{q},q_\perp'} B_{\mathbf{q},q_\perp'}$ includes all photons with in-plane momentum $\mathbf{q}$ in QW m. The term $i\hbar \frac{\partial}{\partial t} \Pi_{\mathbf{k},\mathbf{q},q_\perp,m}|_{\mathrm{scatt}}$ describes Coulomb scattering and phonon-induced three-particle scattering terms.

In order to get a closed set of equations, we need to compute the dynamics of the excitonic correlations which follows from

$$\begin{aligned} i\hbar \frac{\partial}{\partial t} c_{Xm',m}^{\mathbf{q},\mathbf{k}',\mathbf{k}} = {} & \epsilon_{m',m}^{\mathbf{q},\mathbf{k}',\mathbf{k}} c_{Xm',m}^{\mathbf{q},\mathbf{k}',\mathbf{k}} + S_{Xm',m}^{\mathbf{q},\mathbf{k}',\mathbf{k}} - (1 - f_{\mathbf{k}'+\mathbf{q}}^{e,m'} \\ & - f_{\mathbf{k}'}^{h,m'}) \sum_{\mathbf{l}\neq\mathbf{k}'} V_{\mathbf{l}-\mathbf{k}'} c_{Xm',m}^{\mathbf{q},\mathbf{l},\mathbf{k}} + (1 - f_{\mathbf{k}}^{e,m} \\ & - f_{\mathbf{k}-\mathbf{q}}^{h,m}) \sum_{\mathbf{l}\neq\mathbf{k}} V_{\mathbf{l}-\mathbf{k}} c_{Xm',m}^{\mathbf{q},\mathbf{k}',\mathbf{l}} - (1 - f_{\mathbf{k}'+\mathbf{q}}^{e,m'} \\ & - f_{\mathbf{k}'}^{h,m'}) \sum_{q_\perp'} i\mathcal{F}_{m',\mathbf{q}',q_\perp'} (\Pi_{\mathbf{q},q_\perp'}^{\mathbf{k},m})^{\star} - (1 - f_{\mathbf{k}}^{e,m} \\ & - f_{\mathbf{k}-\mathbf{q}}^{h,m}) \sum_{q_\perp'} i\mathcal{F}_{m,\mathbf{q}',q_\perp'}^{\star} \Pi_{\mathbf{q},q_\perp'}^{\mathbf{k}',m'} + i\hbar \frac{\partial}{\partial t} c_{Xm',m}^{\mathbf{q},\mathbf{k}',\mathbf{k}}|_{\mathrm{scatt}}. \end{aligned} \tag{10}$$

Equation (10) yields the consistent form of exciton correlations in the main-sum approximation.[29] It contains the Coulomb-renormalized electron-hole pair energy which is explicitly given by

$$\epsilon_{m',m}^{\mathbf{q},\mathbf{k}',\mathbf{k}} = \tilde{\epsilon}_{\mathbf{k}-\mathbf{q},\mathbf{q}}^{m} - \tilde{\epsilon}_{\mathbf{k}',\mathbf{q}}^{m'}. \tag{11}$$

If the c_X correlation vanishes initially, it is driven by the Coulomb-induced single-particle scattering source

$$\begin{aligned} S_{Xm',m}^{\mathbf{q},\mathbf{k}',\mathbf{k}} = {} & \delta_{m,m'} V_{\mathbf{k}'+\mathbf{q}-\mathbf{k}} \times [f_{\mathbf{k}'+\mathbf{q}}^{e,m} f_{\mathbf{k}'}^{h,m} (1 - f_{\mathbf{k}}^{e,m})(1 - f_{\mathbf{k}-\mathbf{q}}^{h,m}) \\ & - f_{\mathbf{k}}^{e,m} f_{\mathbf{k}-\mathbf{q}}^{h,m} (1 - f_{\mathbf{k}'+\mathbf{q}}^{e,m})(1 - f_{\mathbf{k}'}^{h,m})]. \end{aligned} \tag{12}$$

This source exists only for identical QW indices $m=m'$ and resembles the Coulomb scattering within one and the same QW. Exciton pair-state resonances are introduced by the Coulomb sums in the second and third line of Eq. (10).[29] Additionally, the spontaneous recombination of correlated electron-hole pairs is described by the terms containing Π when $m=m'$. For $m \neq m'$, these terms correlate electron-hole pairs in different QWs due to photon-mediated recombination and excitation of electron-hole pairs. Finally, the last term $i\hbar \frac{\partial}{\partial t} c_{Xm',m}^{\mathbf{q},\mathbf{k}',\mathbf{k}}|_{\mathrm{scatt}}$ includes the Coulomb and phonon scattering contributions due to three-particle correlations.

The incoherent excitation state of the carriers enters the quantum emission via $f^{e,m}$, $f^{h,m}$, and $c_{X,m,m'}$. Thus, the fully self-consistent solution of the MQW PL is obtained by solving the carrier dynamics together with Eqs. (2), (4), and (10). Consequently, we have to set up the equations of motion for the carrier dynamics to close the set of equations. We obtain the equations

$$\begin{aligned} i\hbar \frac{\partial}{\partial t} f_{\mathbf{k}}^{e,m} = {} & \sum_{\mathbf{q},q_\perp} i[\mathcal{F}_{m,\mathbf{q},q_\perp} (\Pi_{\mathbf{q},q_\perp}^{\mathbf{k},m})^{\star} + \mathcal{F}_{m,\mathbf{q},q_\perp}^{\star} \Pi_{\mathbf{q},q_\perp}^{\mathbf{k},m}] \\ & + i\hbar \frac{d}{dt} f_{\mathbf{k}}^{e,m}|_{\mathrm{scatt}} \end{aligned} \tag{13}$$

$$\begin{aligned} i\hbar \frac{\partial}{\partial t} f_{\mathbf{k}}^{h,m} = {} & \sum_{\mathbf{q},q_\perp} i[\mathcal{F}_{m,\mathbf{q},q_\perp} (\Pi_{\mathbf{q},q_\perp}^{\mathbf{k},m})^{\star} + \mathcal{F}_{m,\mathbf{q},q_\perp}^{\star} \Pi_{\mathbf{q},q_\perp}^{\mathbf{k},m}] \\ & - i\hbar \frac{d}{dt} f_{\mathbf{k}}^{h,m}|_{\mathrm{scatt}}, \end{aligned} \tag{14}$$

where the collective sum over all photon-assisted polarization processes determines how strongly electrons and holes recombine spontaneously at momentum $\mathbf{k}$. The last term in Eqs. (13) and (14) defines the Coulomb and phonon induced scattering of carriers.

We notice now that Eqs. (2), (4), and (10) have a structure where different in-plane momenta $\mathbf{q}$ can only be coupled via scattering or by the f^e and f^h dynamics. Additionally in this paper, we concentrate on situations where the carrier states have already experienced significant equilibration. Then, scattering terms can be considered not to produce a $\mathbf{q}$-dependent coupling because f^e and f^h are close to a quasiequilibrium. In this situation, the coupling between different $\mathbf{q}$ in Eqs. (2), (4), and (10) can be ignored. Consequently, the principal MQW coupling effects can be understood by concentrating on the emission in normal direction, i.e., $\mathbf{q}=0$. Under these conditions, $\Pi_{\mathbf{q},q_\perp}$ depends on $\mathbf{q}$ mainly via the angle between the QW and the light field, which leads to a

geometrical factor.[30] Thus, the slow carrier dynamics, Eqs. (13) and (14), is evaluated from $\Pi_{0,q_\perp}$ by applying an appropriate geometrical factor.

In our computations, the steady-state luminescence is proportional to the flux of the photon number

$$I_{PL}(\omega = c|q_\perp|) = \frac{\partial}{\partial t}\Delta\langle B^\dagger_{0,q_\perp} B_{0,q_\perp}\rangle. \tag{15}$$

Furthermore, we may also study the number of excitons with the center of mass momentum $\mathbf{q}=0$ by introducing the transformation

$$\Delta N^{m,m'}_{\nu,\lambda} = \sum_{\mathbf{k},\mathbf{k}'} \phi^L_\nu(\mathbf{k})[\phi^L_\lambda(\mathbf{k}')]^\star c^{0,\mathbf{k}',\mathbf{k}}_{Xm',m}, \tag{16}$$

$$c^{0,\mathbf{k}',\mathbf{k}}_{Xm',m} = \sum_{\nu,\lambda} \Delta N^{m,m'}_{\nu,\lambda}\left[\phi^R_\nu(\mathbf{k})\right]^\star \phi^R_\lambda(\mathbf{k}'), \tag{17}$$

where $\Delta N^{m,m}_{\lambda,\lambda}$ defines the number of excitons in the state λ with center-of-mass momentum $\mathbf{q}=0$ in the QW m. Index combinations with unequal state indices $\lambda \neq \nu$ describe correlated electron-hole plasma contributions and not exciton populations. The transformation (16), (17) is performed by projecting c_X or ΔN onto the left-handed and right-handed excitonic eigenfunctions $\phi^L_\nu(\mathbf{k})$ and $\phi^R_\nu(\mathbf{k})$, respectively.[30] The eigenfunctions can be derived by solving the generalized Wannier equation

$$[\phi^L_\nu(\mathbf{k})]^\star \tilde{\epsilon}_\mathbf{k} - \sum_{\mathbf{k}'} [\phi^L_\nu(\mathbf{k}')]^\star (1 - f^e_{\mathbf{k}'} - f^h_{\mathbf{k}'}) V_{\mathbf{k}-\mathbf{k}'} = [\phi^L_\nu(\mathbf{k})]^\star E_\nu \tag{18}$$

$$\tilde{\epsilon}_\mathbf{k}\phi^R_\nu(\mathbf{k}) - (1 - f^e_\mathbf{k} - f^h_\mathbf{k})\sum_{\mathbf{k}'} V_{\mathbf{k}-\mathbf{k}'}\phi^R_\nu(\mathbf{k}') = E_\nu \phi^R_\nu(\mathbf{k}). \tag{19}$$

For vanishing carrier densities, the Wannier equation has a one-to-one correspondence to the Schrödinger equation for the relative motion problem of the atomic hydrogen.[2] Due to the phase-space filling factor, however, the eigenvalue problem becomes non-Hermitian for finite densities. The solutions yield left- and right-handed eigenfunctions which obey the generalized orthogonality and completeness relation

$$\sum_\mathbf{k} [\phi^L_\nu(\mathbf{k})]^\star \phi^R_\lambda(\mathbf{k}) = \delta_{\nu,\lambda}, \tag{20}$$

$$\sum_\mathbf{k} [\phi^L_\nu(\mathbf{k})]^\star \phi^R_\nu(\mathbf{k}') = \delta_{\mathbf{k},\mathbf{k}'}. \tag{21}$$

One can show that even for finite densities the eigenvalues as well as the eigenfunctions remain real[31] and are related by

$$\phi^L_\nu(\mathbf{k}) = \frac{\phi^R_\nu(\mathbf{k})}{1 - f^e_\mathbf{k} - f^h_\mathbf{k}}. \tag{22}$$

Description of scattering and screening. In the following investigations, we assume the carriers to be close to quasiequilibrium. Hence, we approximate their distributions by Fermi functions with a given temperature and carrier density. In this limit, we can simplify the scattering contributions in Eqs. (4), (10), (13), and (14). The easiest possible approximation is to introduce a constant dephasing γ. This nicely works in the case of the photon-assisted polarization such that we can approximate the scattering term in Eq. (4) by

$$i\hbar \frac{\partial}{\partial t}\Pi^{\mathbf{k},m}_{\mathbf{q},q_\perp}|_{\text{scatt}} = -i\gamma \Pi^{\mathbf{k},m}_{\mathbf{q},q_\perp}. \tag{23}$$

The scattering term in the c_X correlation cannot be treated in that manner since a simple dephasing constant would lead to an unphysical decay of the exciton populations. More specifically, in an exciton basis, we have to distinguish between complex transition amplitudes $\Delta N^{m,m'}_{\nu,\lambda}$ for $\nu \neq \lambda$ or $m \neq m'$ and real-valued populations $\Delta N^{m,m}_{\nu,\nu}$. Since the latter do not carry a phase, they are insensitive to dephasing. They can only decay nonradiatively (not considered here) or via spontaneous emission included in Eq. (10). Therefore, we introduced a scattering term

$$i\hbar \frac{\partial}{\partial t} c^{0,\mathbf{k}',\mathbf{k}}_{Xm',m}|_{\text{scatt}} = -2i\gamma c^{0,\mathbf{k}',\mathbf{k}}_{Xm',m} + 2i\gamma\delta_{m,m'}\sum_\lambda \Delta N^{m,m'}_{\lambda,\lambda}\phi^R_\nu(\mathbf{k}) \times [\phi^R_\lambda(\mathbf{k}')]^\star, \tag{24}$$

which assures that only the off-diagonal correlations are dephased and the diagonal exciton populations stay unaffected. The scattering contributions in the equations of motion (13) and (14) for the carriers can be neglected. Furthermore, Coulomb scattering leads to an effective plasma screening such that the Coulomb matrix element is screened. For this purpose, we use the single-plasmon pole approximation.[2]

The following computations are performed for GaAs-type MQW systems with a QW width of $\Delta L = 8$ nm. For this width we obtain the $1s$-exciton-binding energy $E_B = 10.2$ meV. Additionally, we assume the QWs to be embedded within a spatially homogeneous and optically inactive substrate with constant background refractive index 3.63. We use low carrier densities between $10^7 - 10^9$ cm^{-2} and carrier temperatures between 20 K and 77 K. The homogeneous broadening is set to be $\gamma = 0.42$ meV. As a generic initial condition, the quasiequilibrium QW is populated by different mixtures of electron-hole plasma and exciton distributions.

III. SUBRADIANCE IN MQW SYSTEMS

As a first numerical investigation, we analyze how the luminescence per QW is influenced by the number of QWs in the system. More specifically, we compare the single and 16 QW PL by solving the corresponding steady-state luminescence I_{PL} from Eqs. (2), (4), and (10) when only uncorrelated electron-hole plasma is present, i.e., when the exciton populations are vanishingly small. For this situation, we may neglect the carrier recombination dynamics because it happens on a nanosecond time scale which is slow compared to the picosecond-time scale we are investigating here. We use stationary Fermi-distributed carrier densities $n = 8 \times 10^8$ cm^{-2} and a carrier temperature $T = 77$ K. In order to compare the single and 16 QW photoluminescence, we define a normalized luminescence per QW.

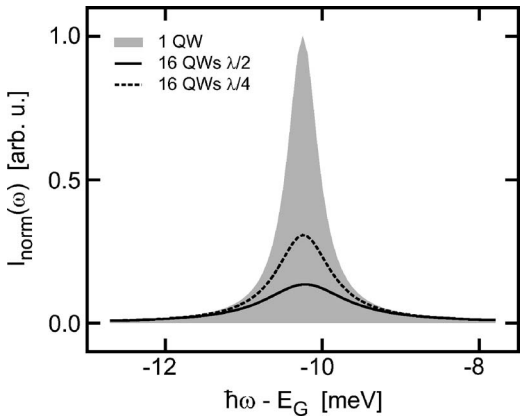

FIG. 1. Steady-state spectra of the luminescence per QW for a single QW (shaded area) and systems of 16 QWs with spacings $\lambda/2$ (solid line) and $\lambda/4$ (dashed line). For these computations, we use $T=77$ K carrier temperature and a Fermi-distributed carrier density of 8×10^8 cm^{-2}.

$$I_{\mathrm{norm}}(\omega) \equiv I_{\mathrm{PL}}(\omega)/N. \tag{25}$$

Figure 1 shows $I_{\mathrm{norm}}(\omega)$ for a single QW (shaded area) and for MQW systems consisting of 16 QWs with a QW separation $\Delta s=\lambda/4$ (dashed line) and $\Delta s=\lambda/2$ (solid line), respectively. The PL per QW is plotted as a function of the energy of the quantum emission. The energy is given relatively to the unrenormalized band gap energy, which is denoted by E_G. We observe that the emission per QW is strongly reduced in MQW systems; this effect is referred to as "subradiance".

As a general trend, subradiance is strongest for the Bragg structures and any detuning of the spacing away from the Bragg-condition leads to a weakening of this effect. The subradiance has a minimum for the QW separation $\lambda/4$ (anti-Bragg spacing) if the number of QWs in the system is even. For odd QW numbers, the minimum is also in the vicinity of the $\lambda/4$ separation but the exact value depends nontrivially on the QW number. To have maximum subradiant effects, we mostly concentrate on Bragg structures in the following. If the carrier densities are increased, the QWs display gain and the coupling effects produce superradiance as shown in Ref. 22. The overall behavior of the emission is clearly different than the decay of the coherent polarization for which the radiative coupling effects produce a superradiant behavior in Bragg structures independent of the carrier density.[12] The difference is a consequence of the fact that the broadening of the coherent spectrum corresponds to a faster (i.e., superradiant) decay of populations whereas the broadening of the spectrum in Fig. 1 is related to the dephasing of Π while the area under the curve determines the total PL.

In order to pinpoint the origin of the subradiance, we have to identify the terms responsible for the QW coupling. In Eq. (4), the only terms which couple different QWs are the recombination correlation Ω_m^{RC} and the stimulated contribution $\Omega^{\mathrm{ST}} \equiv \Delta\langle B^{\dagger}_{\mathbf{q},q_\perp} B_{\mathbf{q}\Sigma_m}\rangle$. We perform a switch-off analysis to investigate the relevance of these two terms for the subradiance of a 16 QWs system. The results of this analysis are

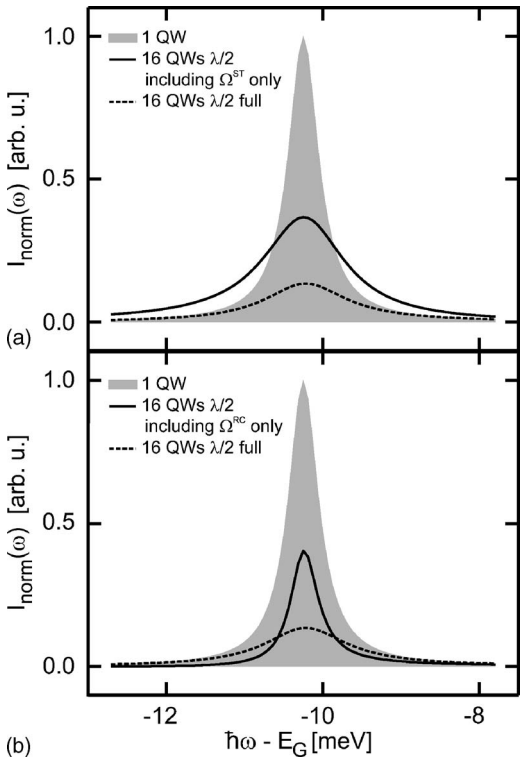

FIG. 2. Origin of subradiance: steady-state spectra for the luminescence per QW comparing the result of a full computation for a single QW (shaded area) and a system of 16 QWs with spacing $\lambda/2$ (dashed line) with the results of a system of 16 QWs with including only the stimulated contribution [solid line in subfigure (a)] and an analogous system with including only the recombination correlation [solid line in subfigure (b)]. The carrier temperature is $T=77$ K and we use a Fermi-distributed carrier density of 8×10^8 cm^{-2}.

depicted in Fig. 2, where we compare the results of a full calculation for a single QW with that of a system of 16 QWs with spacing $\lambda/2$. Additionally, we show in Fig. 2(a) the 16 QW result where only Ω^{ST} is included and in Fig. 2(b) the result where we kept only the Ω_m^{RC} term. The comparisons in Fig. 2 indicate that the stimulated emission term leads to a smaller but broadened resonance peak compared to the single QW result. This effect is clearly analogous to the broadening of a coherent spectrum under superradiant conditions. However, the area under the peak, which determines the total number of emitted photons, remains unchanged. If we only include Ω^{RC} we do not observe a broadening of the resonance but a depletion of the luminescence per QW, i.e., the area under the peak is strongly diminished compared to the single QW emission. Therefore, we conclude that the recombination correlations are dominantly responsible for the subradiance effects.

Since subradiance is a QW-coupling phenomenon it is interesting to see how the strength of the subradiance depends on the number of QWs in the Bragg structure and how Ω^{RC} effects the subradiance. Consequently, we compare the luminescence per QW $I_{\mathrm{norm}}(\omega)$ in the three cases including: (i) the full SLE, (ii) the stimulated contribution only, and (iii) only the recombination correlation. We perform this comparison for Bragg structures with 1 to 10 QWs and use the

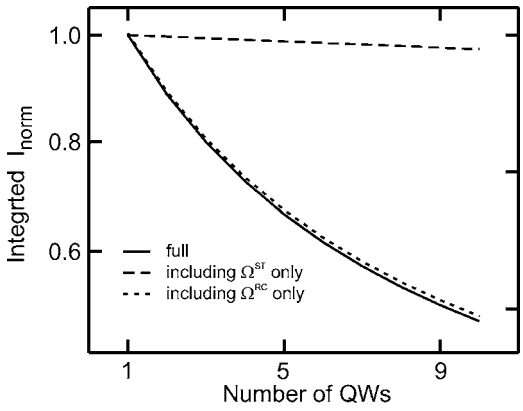

FIG. 3. Strength of subradiance vs QW number: comparison of the integrated luminescence per QW using the full SLE (solid line) against the cases with including only $\Delta\langle B^{\dagger}_{\mathbf{q},q_\perp} B_{\mathbf{q}\Sigma_m}\rangle$ (dashed line) or Ω^{RC} (dotted line) for different numbers of QWs. Carrier temperature and density was the same as in Fig. 2.

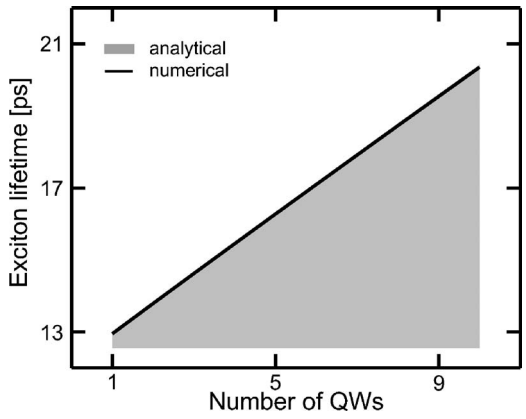

FIG. 4. Excitonic lifetime computed in different Bragg-structured MQW systems. The solid line shows the full numerical result. The shaded area is obtained from a linear extrapolation of the exciton lifetime for 1 and 2 QWs.

same parameters as in the computations before. The results of this analysis are shown in Fig. 3 where the full calculation (solid line) is compared with computations with only Ω^{ST} (dashed line) and Ω^{RC} (dotted line). We observe that the area under the PL peak decreases with increasing QW number, i.e., the effect of subradiance is enhanced.

IV. EXCITON LIFETIME IN MQW SYSTEMS

We investigate next the influence of the MQW structure on the lifetime of bright excitons and analyze how the lifetime is related to the subradiance. Therefore, we introduce the radiative decay constant already known to describe the decay of excitonic polarization[8]

$$\Gamma = \frac{d_{cv}^2 |\phi_{1s}(0)|^2}{2\varepsilon_0 n} q_{1s}. \tag{26}$$

Here, ε_0 is the vacuum dielectric constant, n is the background refractive index and q_{1s} is the photon wave vector corresponding to the exciton energy. The exciton wave function in real space evaluated at $r=0$ is given by $\phi_{1s}(0)$. In single QW systems, the radiative lifetime of coherent excitons, i.e., the square of the polarizations in the classical limit, and the radiative lifetime of bright excitons in the incoherent limit are the same due to the identical structure of the semiconductor Bloch equation and the SLE. Hence, one finds the radiative lifetime of bright excitons in a single QW to be $\tau_1 = \hbar/(2\Gamma)$. The origin of the radiative decay is the recombination of optically active exciton populations, which happens rapidly on a 10 ps time scale. This fast recombination efficiently removes excitons at low momentum states. As a result, the exciton distributions show strong nonequilibrium characteristics[25,30,28] around $\mathbf{q}=0$.

As another general feature, one finds[22] a strict conservation law

$$I_{\mathrm{PL}} = \frac{\partial}{\partial t} \sum_{q_\perp} \Delta\langle B^{\dagger}_{0,q_\perp} B_{0,q_\perp}\rangle = \frac{\partial}{\partial t} \sum_{\mathbf{k}} f^{e,h}_{\mathbf{k}}, \tag{27}$$

which implies that the number of recombined electron-hole pairs equals the number of emitted photons. As the MQW system reduces the total I_{PL} due to subradiance, one simultaneously obtains an enhanced optical lifetime of excitations in the system. Thus, it is interesting to study whether one can apply the subradiance to tailor the radiative lifetime of quasiparticles in semiconductors. The aim here is to determine how one can form an exciton-friendly environment with the help of MQW systems such that the exciton lifetime becomes maximally enhanced.

We know from the investigations in the previous section that the subradiance becomes stronger with larger number of QWs. For that reason, we analyze the influence of the number of QWs on the radiative lifetime of excitons in a Bragg structure by solving Eqs. (2), (4), (10), (13), and (14). In more detail, we initially insert a certain number of excitons into each QW. The carrier density is set to 8×10^8 cm^{-2} and the exciton density is 7.36×10^8 cm^{-2} (exciton fraction is 92%) such that nearly all carriers are present in the form of excitons. The carrier temperature and the homogeneous broadening remain unchanged compared to the previous analysis. The results of this investigation are presented in Fig. 4 where the exciton lifetime is plotted against the QW number for MQW systems with 1 to 10 QWs. The solid line shows the results obtained from the full numerical analysis while the shaded area corresponds to the lifetimes computed with the help of a simplified analytical model discussed in the Appendix. For the analytical investigation, we use the known exciton lifetime τ_1 in a single QW and the result for the exciton lifetime of a 2 QW system calculated by the simplified model. Then, we compute the difference between the lifetimes in these two systems and assume a linear lifetime increase with increasing QW number.

$$\tau_N = \tau_1 + (N-1)\Delta\tau_{12}, \tag{28}$$

where

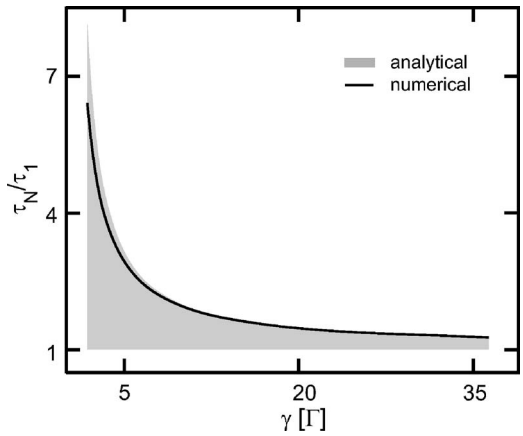

FIG. 5. Exciton lifetime computed for different dephasing constants in Bragg structures with 10 QWs. The solid line shows the full numerical result. The shaded area is the result gained from the analytical approximation presented in the Appendix.

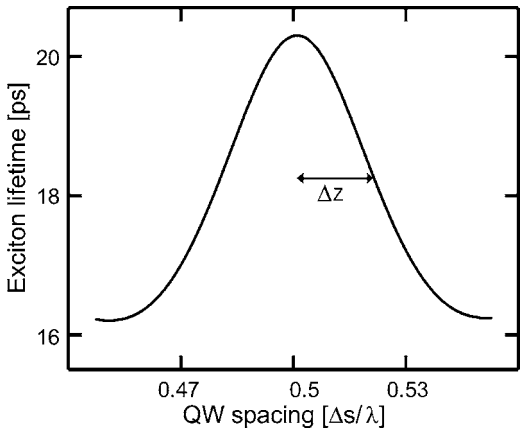

FIG. 6. Exciton lifetime for different QW spacings in a system of 10 QWs. The half width of the resonance around the Bragg condition is denoted by Δz.

$$\Delta\tau_{12} = \tau_1 \frac{\sqrt{\gamma^2 + 4\Gamma^2} - \gamma}{\gamma + 2\Gamma - \sqrt{\gamma^2 + 4\Gamma^2}}. \tag{29}$$

According to Eq. (28), Fig. 4 shows that the lifetime of the full numerical computation rises linearly with increasing QW number. We find that the increase of the exciton lifetime is roughly 0.834 ps per additional QW for the homogeneous γ used in the computations. Furthermore, the simplified model reproduces the lifetimes of the full numerical model very well, although the corresponding analytic calculation only includes exciton contributions. The linear increase of the exciton lifetime with increased QW number corresponds directly to the increase of the subradiance effect. From these observations, we can conclude that the suppression of the photon emission results in an enhancement of the radiative lifetime of excitations in the system. For cases other than $\lambda/2$ spacing, one cannot anymore determine a single decay constant or an exciton lifetime since the decay dynamics consists of several modes with different decay constants.

In addition to the number and spacing of the QWs, the simple formula (29) predicts that the chosen homogeneous broadening of the photoluminescence affects the exciton lifetime. In realistic experiments one can alter γ via the lattice temperature and/or the background carrier density since γ depends on phonon and Coulomb scattering. Note, that the dependence of the exciton lifetime on the homogeneous broadening is introduced by the dephasing constant in the equation of motion for the correlated electron-hole pairs in Eq. (24). Even though, the decay constant is used for off-diagonal exciton correlations only, it influences the radiative decay of diagonal exciton populations via Ω^{RC}. In the following, we analyze this influence for systems of 10 QWs with Bragg-spacing by varying γ for otherwise the same carrier and exciton densities as already used in Fig. 4. The carrier temperature is $T=77$ K and the radiative broadening is $\Gamma=0.025$ meV. In Fig. 5, we show the exciton lifetimes in units of the radiative exciton lifetime in a single QW comparing the results of the full numerical analysis (solid line) and the radiative lifetimes gained by using Eqs. (28) and (29) (shaded area). We find that the lifetime increase becomes stronger for small γ, e.g., we obtain a lifetime of about 76.6 ps for a Bragg structure with 10 QWs and $\gamma=2\Gamma$. For large γ, the QWs become uncoupled such that one recovers the single QW exciton lifetime of about 13 ps. The simplified model predicts the full numerical results very well. For small γ, Eq. (29) slightly overestimates the radiative lifetime increase. This deviation can be explained by additional super-radiant and subradiant modes which occur in a 10 QW system and alter the result slightly for small γ. In a two-QW system these modes are absent and thus not taken into account in the simplified analytical model.

We have already shown in Fig. 1 that the influence of the subradiance is strongest for the Bragg condition. We next investigate the robustness of this subradiance by detuning away from the Bragg spacing. For this purpose, we use the same parameters as in Fig. 4 and plot in Fig. 6 the exciton lifetime for a 10 QW system as a function of spacing. As suggested from the subradiance results, the exciton lifetime is increased strongest in the vicinity of the QW spacing $\lambda/2$. However, we find the maximum lifetime increase at a QW spacing that slightly differs from the exact value of $\lambda/2$. This deviation is a consequence of the emission from exciton populations in states other than $1s$, since these exciton states do not satisfy the Bragg condition. As the spacing is detuned further away from the Bragg condition, the lifetime decreases and reaches a local minimum at a value which depends on the QW number.

In order to compare the sensitivity of the lifetime enhancement under detuning in different MQW structures, we define Δz to be the half-width of the lifetime Bragg resonance, as indicated in Fig. 6. Additionally, we use a simplified model for the SLE introduced in the Appendix of Ref. 22 and extend it, such that exciton populations are taken into account. This analysis allows us to deduce the half width of the Bragg-resonance analytically from

$$\frac{\sin(Nq_{1s}\Delta z)}{\sin(q_{1s}\Delta z)} = \frac{N}{\sqrt{2}}, \tag{30}$$

where q_{1s} is the photon momentum corresponding to the energy of the exciton resonance energy. The number of QWs is

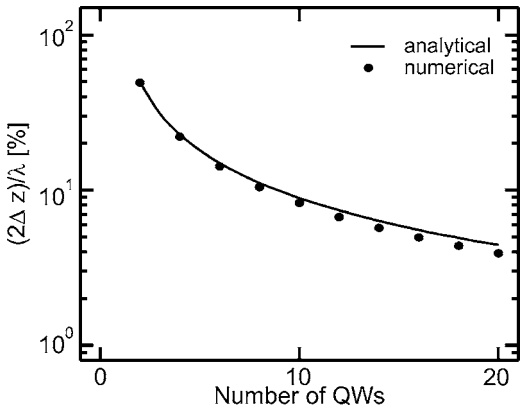

FIG. 7. Half width of the lifetime peak around the Bragg condition for QW arrangements with 2 to 20 QWs. The solid line shows the result gained from Eq. (30) while the filled circles show the full numerical analysis.

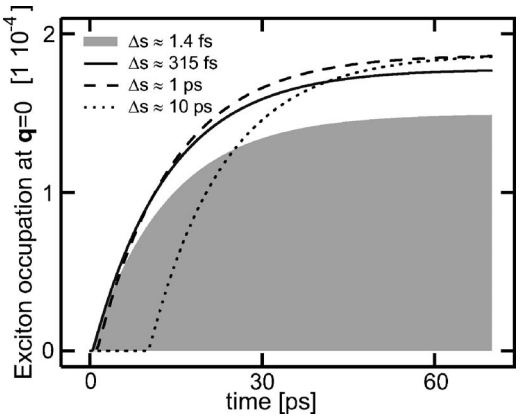

FIG. 8. Excitation of excitons in two radiatively coupled QWs. The first QW is assumed to be populated by a Fermi-distributed carrier density of 3×10^{10} cm^{-2}, while the second QW is initially empty. In the beginning there are no excitons in neither of the two QWs. The exciton occupation at $\mathbf{q}=0$ in the second QW is depicted as a function of time for the four different QW spacings with 1.4 fs$\triangleq\lambda/2$ (shaded area), 0.315 ps (solid line), 1 ps (dashed line), and 10 ps (dotted line) propagation time between the QWs.

denoted by N. The first root of Eq. (30) defines Δz. The result obtained from this formula (solid line) is compared with the full numerical computation (filled circles) for QW arrangements with 2 to 20 QWs in Fig. 7. We observe that the computed half widths excellently agree with those calculated by the numerical analysis of the SLE. Additionally, we find that the shape of the lifetime peak is broad for a small number of QWs and quickly gets sharper for higher numbers of QWs.

V. EXCITON PUMPING

So far, we have demonstrated that the exciton lifetime is strongly influenced by the radiative coupling between different QWs. Since spontaneous emission has its maximum at the exciton resonance, even without the presence of exciton populations, one might ask if this emission may lead to exciton generation in MQW systems. Hence, it is interesting to investigate whether even plasma excitation conditions and plasma luminescence may lead to the formation of excitons directly via radiative coupling. To analyze this basic phenomenon, we study a Bragg structure of two radiatively coupled QWs. We assume that the first QW has an initial carrier density of 3×10^{10} cm^{-2}, while the other QW is unexcited. Additionally, we assume that no exciton populations are present in the beginning. The temperature is chosen to be $T=20$ K and the carrier density in the first QW follows a Fermi distribution. Due to the relatively high density in the first QW, the homogeneous broadening is chosen to be 2.1 meV, according to an excitation-induced dephasing computation.[25] Since the second QW is empty, we use a lower homogeneous broadening of 0.42 meV there. In Fig. 8, the exciton occupation at $\mathbf{q}=0$ for different spacings between the two QWs is presented. The shaded area shows the case where the two QWs are separated by only $\Delta s=\lambda/2$ which corresponds to a 1.4 fs time delay in the light propagation between the QWs. We have also tested other QW distances consisting of integer multiples of $\lambda/2$. The cases where the spacing corresponds to roughly 0.315 (solid line), 1 (dashed line), and 10 ps (dotted line) are also shown in Fig. 8. The exciton distribution at $\mathbf{q}=0$ in the second QW reaches values of about 1.86×10^{-4} which corresponds to an exciton density of about 7.5×10^{4} cm^{-2}. This is not a very high population, but it demonstrates the principle possibility that pure plasma excitations are able to pump excitons in radiatively coupled QWs. The obtained maximum level of pumped excitons can be enhanced considerably by increasing the carrier density in the first QW.

Additionally, we obtain a slight increase in the amount of created excitons for larger QW spacing. This increase stops for QW separations leading to a larger than roughly 0.32 ps delay time, which at the same time matches the dephasing time $\tau_\gamma=\hbar/\gamma=\hbar/(2.1\ \text{meV})$ of the pumping QW. The radiative coupling between QWs is limited by τ_γ, since the QWs become radiatively uncoupled once the QW separation exceeds the spacings corresponding to τ_γ. The homogeneous dephasing in the initially empty QW is much smaller than γ in the pumping QW and therefore its contribution to this effect is only weak.

An interesting feature of the created excitons in the second QW is that all excitons exclusively populate the state of $\mathbf{q}=0$. Detailed investigations[30] show that the excitons in this state show long-range order and reduced phonon and Coulomb scattering. Hence, the excitons are generated in a quantum-degenerate state, i.e., an exciton condensate.

In order to find out whether more plasma-excited QWs may influence the amount of created excitons in a radiatively coupled and initially empty QW, we compare the cases of 2, 3, 5, and 10 QWs with spacings $\lambda/2$. The last QW in both structures is initially empty while the other QWs are initially populated by a Fermi-distributed carrier density of 3×10^{10} cm^{-2}, each. The result of this comparison is shown in Fig. 9. The exciton occupation at $\mathbf{q}=0$ in the second QW of the 2-QW system is depicted by the shaded area. The solid line shows the corresponding occupation in the third QW of the 3-QW system. The cases of 5 and 10 QWs where the last

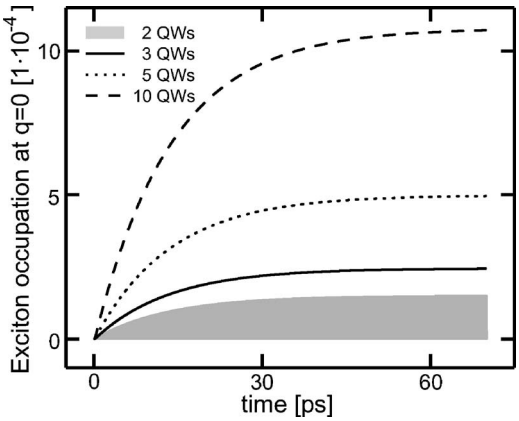

FIG. 9. Exciton occupation at $\mathbf{q}=\mathbf{0}$ of an initially unexcited QW in Bragg-structures with 2 (shaded area), 3 (solid line), 5 (dotted line), and 10 (dashed line) QWs. The other QWs are initially populated by a Fermi-distributed carrier density of 3×10^{10} cm^{-2}.

QW is initially empty are presented by the dotted and the dashed line, respectively. From Fig. 9, we observe that the number of created excitons in the initially empty QW can be strongly increased by using more plasma excited QWs as a source. The amount of created excitons scales nearly linearly with the QW number.

VI. CONCLUSION

Our investigations demonstrate that N QWs can show PL and electron-hole recombination per QW that is reduced with a subradiant dependency on the QW number N. The origin of the subradiance is the recombination of carriers in one QW while a new electron-hole pair is created in another QW at the same time. The subradiance is strongest for the Bragg condition and it increases with increasing number of QWs. This is in sharp contrast to an excitation with classical light, where a supperradiant decay of coherent polarization in Bragg structures is always obtained.

We have found that the radiative lifetime of excitons is directly related to the subradiance in MQW systems such that we obtain a linear dependence of the exciton lifetime on the QW number in Bragg structures. We introduced a simple analytical model that is able to predict the radiative lifetime in Bragg structures for different homogeneous dephasings. For spacings other than $\lambda/2$, such relations are not simple because in these cases several super- and subradiant modes are superimposed such that not only a simple monoexponential or biexponential decay can be observed.

Additionally we have found that a small detuning away from the Bragg condition leads to smaller exciton lifetimes, which is consistent with the subradiance results. We have presented a formula that can be used to determine the half width of the lifetime peaks at the Bragg condition, which very nicely agrees with the results obtained from the full numerical analysis. As a general trend, the lifetime peak becomes sharper for increasing QW number. Additionally, the exciton lifetime is enhanced strongest if the homogeneous dephasing is small. In the limit of very strong dephasing, the QWs become effectively uncoupled and we recover the single QW lifetime.

In MQW systems where one QW is initially unexcited, the radiative coupling between the different QWs provides a mechanism for direct exciton pumping. The creation of the excitons in the initially unexcited QW is such that all excitons are created to the state with vanishing center of mass momentum. Earlier investigations[30] have shown that the excitons in this state have then long-range order and form an exciton condensate. The amount of the created exciton population becomes stronger the more QWs act as a source and the higher the plasma excitation is in the source QWs.

ACKNOWLEDGMENTS

This work was supported by the Deutsche Forschungsgemeinschaft through the Quantum Optics in Semiconductors Research Group.

APPENDIX: ANALYTIC MODEL FOR RADIATIVE LIFETIME IN A 2-QWS SYSTEM

In the following analysis, we investigate the photoluminescence of two QWs via an analytical model. We therefore concentrate on a situation where the photoluminescence is dominated by excitons, i.e., when the uncorrelated plasma source $f^e f^h$ in Eq. (8) can be neglected such that the spontaneous emission reads $\Omega_m^{\mathrm{SE}}(\mathbf{k},\mathbf{q})=\Sigma_{\mathbf{l}}\mathcal{F}_{m,\mathbf{q},q_\perp}c^{\mathbf{q},\mathbf{k},\mathbf{l}}_{Xm,m}$. As a first step we can transform Eq. (4) into the exciton picture using the transformation (16) and additionally the relation

$$\Pi^{\mathbf{k},m}_{\mathbf{q},q_\perp}=\sum_\nu \tilde{\Pi}^{m,\nu}_{\mathbf{q},q_\perp}\phi_\nu(\mathbf{k}). \tag{A1}$$

We concentrate on 1s-exciton contributions only and drop the superscript $\nu=1s$ for notational simplicity. We obtain the result

$$\begin{aligned} i\hbar\frac{\partial}{\partial t}\tilde{\Pi}^m_{\mathbf{q},q_\perp}(t)=&(\tilde{\epsilon}_1-\hbar\omega_{\mathbf{q}}-i\gamma)\tilde{\Pi}^m_{\mathbf{q},q_\perp}(t)\\ &-\sum_{q'_\perp}\mathcal{F}^{1s}_{m,\mathbf{q},q'_\perp}\Delta\langle B^\dagger_{\mathbf{q},q_\perp}B_{\mathbf{q},q'_\perp}\rangle(t)\\ &+\sum_n i\mathcal{F}^{1s}_{n,\mathbf{q},q_\perp}N^{\mathbf{q}}_{m,n}(t), \end{aligned} \tag{A2}$$

where $\tilde{\epsilon}_1$ is the $1s$ eigenenergy and $\mathcal{F}^{1s}_{m,\mathbf{q},q_\perp}\equiv d_{cv}\mathcal{E}_q U_{m,\mathbf{q},q_\perp}\Phi^\star_{1s}(r=0)$ with $\Phi_{1s}(r=0)$ being the $1s$-exciton wave function in real space at $r=0$. We switch on the optical coupling at time $t=0$ and assume the excitonic correlations (10) to be constant for negative times. For positive times, the correlations are determined by the radiative coupling between the QWs. In order to eliminate the dependence of Eq. (A2) on the $\Delta\langle B^\dagger B\rangle$, we formally solve Eq. (2) assuming the absence of any external source and insert the result in Eq. (A2). After an additional Fourier transform, we obtain

$$(\hbar\Omega - \epsilon_1 + \hbar\,\omega_{\mathbf{q}} + i[\gamma+\Gamma])\tilde{\Pi}^m_{\mathbf{q},q_\perp}(\Omega)$$
$$= -i\Gamma \sum_{n\neq m} \tilde{\Pi}^m_{\mathbf{q},q_\perp}(\Omega) e^{i(\omega_{\mathbf{q}+\Omega})\tau_{n,m}}$$
$$+ \sum_n i\mathcal{F}^{1s}_{n,\mathbf{q},\mathbf{q}_\perp} N^{\mathbf{q}}_{m,n}(t=0)\,\delta(\Omega)$$
$$+ \sum_n i\mathcal{F}^{1s}_{n,\mathbf{q},q_\perp} N^{\mathbf{q}}_{m,n}(\Omega), \tag{A3}$$

with the radiative lifetime Γ defined by Eq. (26). The retardation time is defined by $\tau_{n,m}=|z_n-z_m|/c$ where z_n and z_m are the positions of the 2 QWs in real space and c is the speed of light. Analogously, we transform Eq. (10) into

$$[\hbar\Omega + i2\gamma(1-\delta_{m,n})]N^{\mathbf{q}}_{m,n}(\Omega) = -\sum_{\mathbf{q}} i\mathcal{F}^{1s}_{m,\mathbf{q},q_\perp}[\tilde{\Pi}^n_{\mathbf{q},q_\perp}]^\star(\Omega)$$
$$-\sum_{\mathbf{q}} i[\mathcal{F}^{1s}_{n,\mathbf{q},q_\perp}]^\star \tilde{\Pi}^m_{\mathbf{q},q_\perp}(\Omega). \tag{A4}$$

We solve Eq. (A3) and insert the result into Eq. (A4). For that purpose, we assume that initially the exciton populations in the first QW $N_{1,1}$ and the second QW $N_{2,2}$ are identical and that there are no initial electron-hole correlations $N_{1,2}$ and $N_{2,1}$ between the two QWs, such that

$$N^{\mathbf{q}}_{1,1}(t=0) = N^{\mathbf{q}}_{2,2}(t=0) = N_{\mathbf{q}},$$

$$N^{\mathbf{q}}_{1,2}(t=0) = N^{\mathbf{q}}_{2,1}(t=0) = 0.$$

If we choose the QW spacing to be $\Delta s=\lambda/2$, the populations in both QWs as well as both correlations remain identical for all times such that we end up with a set of two equations. Taking into account that only exciton populations or electron-hole correlations with vanishing center-of-mass momentum contribute to the coupling of the QWs, we find the relation

$$\begin{pmatrix} \hbar\Omega_E & -2i\Gamma \\ -2i\Gamma & \hbar\Omega_O \end{pmatrix}\begin{pmatrix} N_{11}(\Omega) \\ N_{12}(\Omega) \end{pmatrix} = \begin{pmatrix} -2\Gamma\,\delta(\Omega)N_{\mathbf{q}=0} \\ -4\Gamma\,\delta(\Omega)N_{\mathbf{q}=0} \end{pmatrix}, \tag{A5}$$

with $\hbar\Omega_E=\hbar\Omega+2i\Gamma$ and $\hbar\Omega_O=\hbar\Omega+2i\Gamma+2\gamma$. Diagonalizing the matrix and retransforming the results for the exciton populations into time domain yields one super-radiant and one subradiant solution. The time evolution of the excitons in both QWs is then proportional to

$$N(t) \propto \Theta(t)[A\cdot e^{-(\lambda_+ t)/\hbar} + B\cdot e^{-(\lambda_- t)/\hbar}], \tag{A6}$$

where A and B are γ- and Γ-dependent prefactors. The decay constants are defined by

$$\lambda_\pm = \gamma + 2\Gamma \pm \sqrt{\gamma^2+4\Gamma^2}. \tag{A7}$$

Thus, the plus sign denotes the superradiant mode while the minus sign denotes the subradiant mode. The radiative lifetimes corresponding to these two modes are given by

$$\tau_2(\pm) = \hbar/\lambda_\pm. \tag{A8}$$

Comparing this result to the exciton lifetime obtained in a single QW, we find the lifetime difference

$$\Delta\tau_{12}(\pm) = \tau_2(\pm) - \tau_1 = \tau_1 \frac{\mp\sqrt{\gamma^2+4\Gamma^2}-\gamma}{\gamma+2\Gamma\pm\sqrt{\gamma^2+4\Gamma^2}}. \tag{A9}$$

The full analysis with the help of Eqs. (2), (4), (10), (13), and (14) shows that for early times the superradiant mode dominates the decay of the exciton population but after some picoseconds the subradiant mode overtakes and determines the decay.

*Electronic address: martin.schaefer@physik.uni-marburg.de

[1] E. Hanamura, Phys. Rev. B **38**, 1228 (1988).
[2] H. Haug and S. W. Koch, *Quantum Theory of the Optical and Electronic Properties of Semiconductors* (World Scientific, Singapore, 2004), 4th ed.
[3] J. J. Hopfield, Phys. Rev. **112**, 1555 (1958).
[4] V. M. Agranovich and O. A. Dubowskii, JETP Lett. **3**, 223 (1966).
[5] M. Kira, F. Jahnke, and S. W. Koch, Phys. Rev. Lett. **81**, 3263 (1998).
[6] S. Chatterjee, C. Ell, S. Mosor, G. Khitrova, H. M. Gibbs, W. Hoyer, M. Kira, S. W. Koch, J. P. Prineas, and H. Stolz, Phys. Rev. Lett. **92**, 067402 (2004).
[7] L. C. Andreani, F. Tassone, and F. Bassani, Solid State Commun. **77**, 641 (1991).
[8] J. Feldmann, G. Peter, E. O. Göbel, P. Dawson, K. Moore, C. Foxon, and R. J. Elliott, Phys. Rev. Lett. **59**, 2337 (1987).
[9] B. Deveaud, F. Clérot, N. Roy, K. Satzke, B. Sermage, and D. S. Katzer, Phys. Rev. Lett. **67**, 2355 (1991).
[10] R. H. Dicke, Phys. Rev. **93**, 99 (1954).
[11] Y. C. Lee and P. S. Lee, Phys. Rev. B **10**, 344 (1974).
[12] S. Haas, T. Stroucken, M. Hübner, J. Kuhl, B. Grote, A. Knorr, F. Jahnke, S. W. Koch, R. Hey, and K. Ploog, Phys. Rev. B **57**, 14860 (1998).
[13] B. Laikhtman and L. D. Shvartsman, Phys. Rev. B **72**, 245333 (2005).
[14] B. I. Mantsyzov, Phys. Rev. A **51**, 4939 (1995).
[15] B. I. Mantsyzov, I. V. Mel'nikov, and J. S. Aitchison, IEEE J. Quantum Electron. **10**, 893 (1995).
[16] I. V. Mel'nikov, J. S. Aitchison, and B. I. Mantsyzov, Opt. Lett. **29**, 289 (2004).
[17] T. Stroucken, A. Knorr, P. Thomas, and S. W. Koch, Phys. Rev. B **53**, 2026 (1996).
[18] M. Hübner, J. P. Prineas, C. Ell, P. Brick, E. S. Lee, G. Khitrova, H. M. Gibbs, and S. W. Koch, Phys. Rev. Lett. **83**, 2841 (1999).
[19] T. Shih, K. Reimann, M. Woerner, T. Elsaesser, I. Waldmuller, A. Knorr, R. Hey, and K. H. Ploog, Phys. Rev. B **72**, 195338 (2005).
[20] I. Waldmueller, W. W. Chow, and A. Knorr, Phys. Rev. B **73**, 035433 (2006).
[21] Y. Merled'Aubigné, A. Wasiela, H. Mariette, and T. Dietl, Phys. Rev. B **54**, 14003 (1996).

[22] M. Kira, F. Jahnke, W. Hoyer, and S. W. Koch, Prog. Quantum Electron. **23**, 189 (1999).
[23] H. W. Wyld and B. D. Fried, Ann. Phys. (N.Y.) **23**, 374 (1963).
[24] J. Fricke, Ann. Phys. (N.Y.) **252**, 479 (1996).
[25] M. Kira and S. W. Koch, Eur. Phys. J. D **36**, 143 (2005).
[26] W. Hoyer, M. Kira, and S. W. Koch, Adv. Solid State Phys. **42**, 55 (2002).
[27] W. Hoyer, C. Ell, M. Kira, S. W. Koch, S. Chatterjee, S. Mosor, G. Khitrova, H. M. Gibbs, and H. Stolz, Phys. Rev. B **72**, 075324 (2005).
[28] S. W. Koch, M. Kira, G. Khitrova, and H. M. Gibbs, Nat. Mater. (to be published).
[29] W. Hoyer, M. Kira, and S. W. Koch, Phys. Rev. B **67**, 155113 (2003).
[30] M. Kira and S. W. Koch, Phys. Rev. A **73**, 013813 (2006).
[31] Complex eigenvalues and eigenfunctions can appear if the Coulomb scattering is included microscopically via k-dependent complex scattering matrices. In those cases, the relation (22) does not hold any more [see cond-mat/0604349 (unpublished)].